

Contract No:

This document was prepared in conjunction with work accomplished under Contract No. DE-AC09-08SR22470 with the U.S. Department of Energy.

Disclaimer:

This work was prepared under an agreement with and funded by the U.S. Government. Neither the U. S. Government or its employees, nor any of its contractors, subcontractors or their employees, makes any express or implied: 1. warranty or assumes any legal liability for the accuracy, completeness, or for the use or results of such use of any information, product, or process disclosed; or 2. representation that such use or results of such use would not infringe privately owned rights; or 3. endorsement or recommendation of any specifically identified commercial product, process, or service. Any views and opinions of authors expressed in this work do not necessarily state or reflect those of the United States Government, or its contractors, or subcontractors.



1

2

Upward Movement of Plutonium to Surface Sediments

3

During an 11-Year Field Study

4

5

6 Kaplan, D. I.,*^a D. I. Demirkanli,^b F. J. Molz,^b D. M. Beals,^a J. R. Cadieux, Jr.,^a and J. E. Halverson^a

7

8

9 * Corresponding author phone: 803-725-2363; fax: 803-725-4704; e-mail:

10 daniel.kaplan@srnl.doe.gov.

11 ^a Savannah River National Laboratory, Aiken, SC 29808 USA

12 ^b Clemson University, Environmental Engineering and Earth Sciences, Clemson, SC USA

13

14

15 **Keywords:** Plutonium; Thermal ionization mass spectroscopy; TIMS; Plants; Vadose zone;

16 Concentration ratio; Isotopes

17
18
19
20
21
22
23
24
25
26
27
28
29
30
31
32
33
34
35
36
37
38

Upward Movement of Plutonium to Surface Sediments During an 11-Year Field Study

Abstract

An 11-y lysimeter study was established to monitor the movement of Pu through vadose zone sediments. Sediment Pu concentrations as a function of depth indicated that some Pu moved upward from the buried source material. Subsequent numerical modeling suggested that the upward movement was largely the result of invading grasses taking up the Pu and translocating it upward. The objective of this study was to determine if the Pu of surface sediments originated from atmosphere fallout or from the buried lysimeter source material (weapons-grade Pu), providing additional evidence that plants were involved in the upward migration of Pu. The $^{240}\text{Pu}/^{239}\text{Pu}$ and $^{242}\text{Pu}/^{239}\text{Pu}$ atomic fraction ratios of the lysimeter surface sediments, as determined by Thermal Ionization Mass Spectroscopy (TIMS), were 0.063 and 0.00045, respectively; consistent with the signatures of the weapons-grade Pu. Our numerical simulations indicate that because plants create a large water flux, small concentrations over multiple years may result in a measurable accumulation of Pu on the ground surface. These results may have implications on the conceptual model for calculating risk associated with long-term stewardship and monitored natural attenuation management of Pu contaminated subsurface and surface sediments.

1. Introduction

40

41 The long-term behavior of Pu in the environment is becoming increasingly important as we
42 enter into new phases of the lifecycle of Pu: disposal, recycling into fuel, and remediation of Pu
43 contaminated environments. Plutonium in high-level waste tanks is being vitrified and will be
44 eventually disposed in a deep national repository. Plutonium in low-level waste is being
45 disposed at various shallow vadose-zone facilities. Some pure forms of Pu will be recycled by
46 converting into mixed oxide fuels (or MOX) for use in electrical nuclear power plants. During
47 the production of Pu between the 1950s through the 1980s environmental contamination
48 occurred at several Department of Energy sites, including Los Alamos National Laboratory,
49 Hanford Site, Idaho National Laboratory, Oak Ridge National Laboratory, and the Savannah
50 River Site (Riley and Zachara, 1992). These Pu-contaminated sites have been or will be
51 remediated. In some cases, contaminated sediments have been excavated and treated elsewhere,
52 whereas at other contaminated sites, amendments are mixed into the sediment to reduce the
53 bioavailability or movement of the Pu. But perhaps most commonly, sites contaminated with
54 low concentrations of Pu will be left intact and its movement will be monitored through a long-
55 term monitoring and natural attenuation plan. In all three remediation approaches, some Pu will
56 be left in the ground, and the management of Pu in the environment must be based on sound,
57 long-term science.

58 Four lysimeters were established on the Savannah River Site (SRS) located in Aiken, South
59 Carolina, USA to evaluate the long-term transport of Pu through vadose zone sediments
60 (described in Kaplan et al., 2004; 2006; 2007). The lysimeters consisted of inverted 52-L
61 bottomless carboys that were connected to separate leachate collection reservoirs. The
62 lysimeters were filled with well-mixed subsurface sediment and amended with approximately 1.7

63 $\times 10^7$ Bq (3.4×10^{-5} mol) of Pu, added as $\text{Pu}^{\text{IV}}(\text{NO}_3)_4$, $\text{Pu}^{\text{IV}}(\text{C}_2\text{O}_4)_2$, $\text{Pu}^{\text{III}}\text{Cl}_3$, or $\text{Pu}(\text{OH})_4$. The Pu
64 sources existed as solids and were placed 22 cm below the surface. The lysimeters were initiated
65 in 1981 and were exposed to natural weather conditions (average = 122 cm y^{-1} precipitation) for
66 11 years. The test plan called for grass (weeds) found growing in the lysimeters to be cut and the
67 biomass left on the lysimeter surface (avoiding a potential radioactive waste disposal problem).
68 Vertical sediment cores were collected from the center of the lysimeters and then these cores
69 were cut up into 1.25- or 2.5-cm thick depth-discrete samples. Total $^{239/240}\text{Pu}$ concentrations
70 were measured by alpha spectrometry in each sample.

71 Sediment cores recovered from these lysimeters revealed that a significant portion of the Pu
72 moved upward (Figure 1). Pu downward movement was well described by a fully transient
73 reactive transport model that took into consideration transient sediment moisture saturation,
74 steady state Pu sorption, and kinetic terms to describe Pu(IV) oxidation to Pu(V) and Pu(V)
75 reduction to Pu(IV) (Demirkanli et al., 2007). However, this same model could not describe Pu
76 upward movement (Demirkanli et al., 2008). For a range of sediment properties, these
77 simulations showed that the upward soil water flux due to evapotranspiration, which accounted
78 for about 1/2 to 2/3 of the water that entered the lysimeters, was not sufficient to explain the
79 observed upward movement of Pu. Further computer testing permitted us to eliminate several
80 other potential chemical and hydraulic processes, including one in which Pu became more
81 oxidized (and mobile) as the sediment's moisture-content decreased; adjusting the hypothetical
82 root-distribution to favor upward fluxes of water; and considering hysteresis, caused higher
83 hydraulic conductivities in the sediment for a drying condition than a wetting condition.
84 Following these studies, Demirkanli et al. (2009) concluded that the upward movement of Pu
85 was the likely result of Pu root uptake and translocation within the transpiration (xylem) pathway.

86 This conclusion was based on computer simulations that produced successful modeling of Pu
87 xylem transport using physically meaningful plant and sediment parameters.

88 In two of the three Pu core profiles, the profiles amended with $\text{Pu}(\text{NO}_3)_4$ and PuCl_3 , a slight
89 increase in sediment Pu concentrations were noted in the surface 2.5-cm thick samples (Figure 1).

90 This increase in surface sediment Pu concentrations could be attributed to either atmospheric
91 deposition, or to plant material depositing Pu to the surface sediment as a result of annual die
92 back. If the latter was true, then it would provide direct evidence in support of the conclusion by
93 Demirkanli et al. (2009) that Pu upward movement was due to plant uptake and subsequent
94 redistribution in the sediment profile. Another possibility was that earthworms were responsible
95 for the upward Pu movement. We ruled out bio-perturbation, such as earthworm activity, based
96 on two observations: 1) after careful inspection, no earthworm galleys or other animal activities
97 were found in the sediment cores, and 2) the shape of the Pu depth profiles in Figure 1 were not
98 like those of a bio-perturbed system. Bio-perturbed systems characteristically show the surface
99 sediment layers with an erratic concentration profile down to the depth where the worms exist.

100 These Pu concentration profiles, especially for the PuCl_3 and $\text{Pu}(\text{C}_2\text{O}_4)_2$, show a rather
101 symmetrical shape above and below the source, with most of the scatter of the data occurring at
102 low sediment-Pu concentrations.

103

104 **1.1 Plant Uptake**

105 Plutonium exists in four oxidation states in the natural environment, +3, +4, +5 and +6 (Silva
106 and Nitsche, 1995). The oxidized forms are appreciably more soluble and mobile in sediments
107 than the reduced forms. Pu(V) and Pu(VI) have been shown to undergo rapid reduction by
108 numerous mineral surfaces. Thus, most of the Pu in sediments exists in the reduced form, even

109 in surface sediments with seemingly oxidizing conditions (Powell et al. 2005). Plant uptake of
110 sediment Pu is extremely limited with surprisingly similar concentration ratios (ratio of the
111 concentration in above-ground plant to the concentration in sediment) reported in the literature,
112 ranging from 10^{-5} to 10^{-4} for a wide range of plants and sediments [reviewed by Wang et al.,
113 1993).

114 Cataldo et al. (1988) reported that Pu in the xylem of soybean plants (Glycine max (L.))
115 existed almost exclusively as an organic complex. Pu^{+4} in the uncomplexed form was
116 immediately and strongly retained by the xylem and did not translocate within the plant.
117 Wildung and Garland (1974) observed from autoradiographs of barley (Hordeum vulgare var.
118 Vanguard) that Pu was evenly distributed within the roots and tended to concentrate in the crown.
119 They concluded that although Pu may be strongly bound to sediments, the little amount of Pu
120 that entered the plant was readily distributed through the root system as an organo-Pu complex,
121 moving both upward and downward in the root profile. Furthermore, they concluded that the
122 potential exists for decomposing roots to be a significant source of Pu of different solubility than
123 the Pu that originally entered the soil environment. It is possible that the observed increases of
124 Pu uptake with successive plantings of clover during a 10 year field study resulted from this
125 latter phenomenon (Romney et al., 1970).

126 Plants have been shown to enhance sediment metal and radionuclide bioavailability through
127 the release of root exudates, including phytosideraphores (Bais et al., 2006; Rengel and Romheld,
128 2000) and release of siderophores from root-associated microbes (Bar-Ness et al., 1992). The
129 presence of these plant-derived organic molecules can behave as ligands, increasing Pu solubility,
130 especially for Pu(III) and Pu(IV). Additionally, microbial populations increase in the
131 rhizosphere, the organic carbon rich root environment, and play important direct (metabolize) or

132 indirect (release of extracellular polymeric substances) roles influencing metal/radionuclide
133 phytoavailability.

134 There are very few examples in the literature of clearly documented upward movement of
135 radionuclides in systems where the net movement of soil water is downward. Sanford et al.
136 (1998) reported that Cs and Sr may have moved upward 100 cm during a 10 year field lysimeter
137 study conducted at the Oak Ridge National Laboratory. In a recovered vertical sand core, they
138 observed a root of an unidentified plant. The root had ^{137}Cs concentrations that were about 1.5
139 orders-of-magnitude greater than the bulk sand concentrations. The sand ^{137}Cs concentrations
140 decreased sharply away from the root. They concluded that the root was responsible for the
141 observed upward movement of ^{137}Cs .

142

143 **1.2 Atmospheric deposition of plutonium**

144 Plutonium originating from atmospheric nuclear weapons testing is the largest source of Pu
145 to the environment and can be detected throughout the earth's surface, with the greatest
146 concentration existing in the northern hemisphere and the lowest in Antarctica (Harley 1980;
147 Perkins and Thomas, 1980). Differences in weapons design and yield account for much of the
148 variability measured in the $^{240}\text{Pu}/^{239}\text{Pu}$ isotopic ratios of fallout Pu (Perkins and Thomas, 1980).
149 For example, the average global fallout $^{240}\text{Pu}/^{239}\text{Pu}$ ratio is 0.18, where the ratio from the Nevada
150 Test Site is generally lower, averaging 0.035. Higher ratios can be generally expected with the
151 higher neutron fluxes associated with an increase in the yield of a nuclear detonation, and will
152 vary with weapons design. Such elevated ratios have been measured in environmental samples
153 impacted by nuclear weapons testing in the Pacific (Koide et al., 1983). Therefore, the relative
154 abundances of ^{239}Pu , ^{240}Pu , and other minor Pu isotopes such as ^{241}Pu and ^{242}Pu can be used to

155 trace the specific Pu source because Pu isotopic ratios can vary with reactor type, nuclear fuel
156 burn-up time, and neutron flux and energy (Beasley et al., 1981; Buesseler, 1997).

157 The hypothesis of the present study is that the surface accumulation of Pu was the result of
158 Pu being taken up by plant roots, translocated to the above-ground portion of the plants, and then
159 deposited as plant detritus on the ground surface. This hypothesis was prompted by three
160 observations: 1) elevated total Pu concentrations in some surface sediment samples collected at
161 the lysimeter, 2) the intermittent presence of grasses growing on the lysimeters (Andropogon
162 virginicus, broomsedge; Paspalum notatum, Bahia grass; and Digitaria sp., crabgrass), and 3)
163 modeling results (Demirkanli et al. (2009) suggesting that a substantial amount of Pu could be
164 taken up by lysimeter plants during the 11 year experiment. Thus, the objective of this study was
165 to determine whether the source for the Pu in the surface sediment samples was from
166 atmospheric deposition or the underlying weapons-grade Pu materials added to each lysimeter.
167 Our approach was to compare Pu isotopic ratios of the lysimeter surface sediments with those of
168 two types of controls: a positive control for the weapons-grade Pu buried in the lysimeters (a
169 lysimeter sediment sample collected from within 6 cm of the $\text{Pu}^{\text{IV}}(\text{NO}_3)_4$ buried source material),
170 and two positive controls for atmospheric deposition. Plutonium isotopic ratios were determined
171 by thermal ionization mass spectroscopy (TIMS), an extremely sensitive method for detecting
172 isotopes with detection limits in the order of $0.2 \text{ fg g}^{-1} {}^{239}\text{Pu}$ or $8 \times 10^{-19} \text{ mole g}^{-1} {}^{239}\text{Pu}$. Such low
173 detection limits are the result of including several internal analytical sample controls, using large
174 volumes of sample (up to 20 g per sample for the fallout control samples in this study), the use of
175 a sensitive instrument housed in a Class 10,000 clean room, and perhaps most importantly final
176 sample loading in a Class 1000 hood. In addition to conducting TIMS analyses, we also
177 conducted numerical simulations to describe the impact that plants may have on Pu

178 concentrations in a lysimeter sediment profile. The model was also used to predict Pu uptake by
179 lysimeter grasses and subsequent distribution within roots and transfer into shoots over the
180 duration of the lysimeter experiment, 11 years.

181

182 **2. Materials and methods**

183

184 **2.1 Sediment samples**

185 A total of seven sediment samples were analyzed by TIMS for ^{239}Pu , ^{240}Pu , ^{241}Pu , and ^{242}Pu :
186 four lysimeter surface sediments, one positive control for the weapons-grade Pu, and two
187 positive controls for atmospheric fallout. The two fallout control samples were expected to
188 contain varying Pu isotopic ratios by virtue of their varying distance from the SRS, a former
189 weapons production facility: one sample was collected on the Savannah River Site perimeter, 16
190 km from the lysimeter field site, and the second sample was collected from Anderson, South
191 Carolina, USA 190 km from the lysimeter field site. The positive control for the weapons-grade
192 Pu, the Pu source material buried in the four lysimeters, was collected 6 cm below the
193 $\text{Pu}^{\text{IV}}(\text{NO}_3)_4$ source; it contained $14.15 \text{ Bq g}^{-1} \text{ }^{239/240}\text{Pu}$ and $0.25 \text{ Bq g}^{-1} \text{ }^{238}\text{Pu}$. Prior to preparing
194 the sediments for TIMS analysis, the visible organic matter, including forest litter and roots, was
195 removed from the fallout control samples. No organic matter was visibly present in the other
196 five samples. All samples were passed through a 2-mm sieve.

197 The lysimeter sediment has been described previously (Kaplan et al., 2004). Briefly, it has a
198 sandy loam texture, a 1:1 sediment:water pH of 6.3, and no measurable organic matter. Its red
199 color is derived from the high concentration of iron-(oxy)hydroxides, especially hematite, which
200 showed a strong presence in X-ray diffraction and Mössbauer measurements. The high total Fe

201 concentrations ($15,888 \text{ mg kg}^{-1}$) and low Fe(II) / Fe(III) ratios (1.9% / 98.1%) are typical of
202 vadose zone sediments of this region. In apparent contradiction with the oxidizing nature of the
203 Fe-oxyhydroxides, this sediment can quickly reduce Pu(V) to Pu(IV) (Kaplan et al., 2004).
204 Sediment Mn concentrations, a potential oxidizing or reducing agent, are low at about 630 mg
205 kg^{-1} .

206

207 **2.2 Thermal Ionization Mass Spectroscopy Analyses (TIMS)**

208 A description of the sample preparation protocol is presented in Landa et al. (1998) and a
209 description of the TIMS instrument is presented in Halverson (1981) and Buessler and
210 Halverson (1987). A 1 to 20 g sediment sample was analyzed. A 0.002 Bq (0.06 pCi) aliquot of
211 ^{242}Pu was added to some of the samples (the two fallout control samples) to provide an internal
212 standard for quantifying Pu isotope concentrations by mass spectroscopy. However, ^{242}Pu was
213 not added to all samples because $^{242}\text{Pu}/^{239}\text{Pu}$ atomic mass ratios were of interest. Quantification
214 of $^{239/240}\text{Pu}$ and ^{238}Pu concentrations was provided by alpha spectrometry analyses on a separate
215 aliquot. The samples were then leached with hot 8 M nitric acid and hydrogen peroxide for
216 several hours. The slurry was transferred to a centrifuge tube and the undigested residue
217 separated from the supernate. The supernate was taken to near dryness and then diluted with
218 deionized water. Initial separation from the matrix ions and U was achieved by precipitating
219 hydroxides of iron from a carbonate rich solution; ammonium hydroxide was added to the
220 solution until a pH of about 5, and then a saturated solution of ammonium carbonate was added
221 to a pH of 8. The precipitate with entrained Pu was separated by centrifugation and the
222 supernate discarded.

223 Several ion exchange separation columns were used to purify the Pu prior to mass
224 spectrometry analysis. For the first column separation, the Pu was reduced to the +4 oxidation
225 state using NaNO_2 in 8 M nitric acid and then recovered with a 20 mL column using an 8%
226 cross-linked anion exchange resin (AG 1X8). Interfering elements were washed through the
227 column and the Pu finally eluted after reduction to the +3 state with $\text{NH}_4\text{I}/\text{HCl}$. The eluant
228 containing the Pu was taken to dryness, converted to the +4 oxidation state and passed through a
229 5 mL bed volume, 4% cross-linked, anion exchange column (AG 1X4). The column purification
230 was repeated once more using only a 0.5 mL bed volume of the 4% cross-linked resin, using HBr
231 to ultimately elute the Pu. This final purified sample was then analyzed by TIMS.

232 Plutonium was sorbed onto a few resin beads which were then mounted onto a canoe shaped
233 rhenium- ribbon filament for the instrumental analysis. The three-stage TIMS analyzer
234 (Halverson, 1987) was used for the analysis rather than the single-sector TIMS analyzer (Landa
235 et al., 1998) in order to provide values for the Pu isotopes of lower abundance, ^{241}Pu and ^{242}Pu .
236 The three-sector TIMS analyzer consists of two identical magnetic analyzers in a C-
237 configuration followed by an electrostatic analyzer and an ion-multiplier type detector. As noted
238 above, this instrument is housed in a Class 10,000 clean-room facility. Filament fabrication and
239 sample loading is performed in laminar flow hoods rated at Class 1000.

240 Typical recoveries for the analysis of Pu in soil and sediment by this procedure average
241 between 75 to 90% as determined by the analysis of the ^{242}Pu spiked samples. Calculated
242 detection limits are on the order of 0.2 fg/g (0.5 $\mu\text{Bq/g}$) for ^{239}Pu , based on the analysis of reagent
243 blanks. The NIST Columbia River sediment (SRM 4334G) was used as a Quality Control
244 samples for accuracy and precision. The NIST Columbia River sediment is certified for $7.6 \pm$
245 $2.1 \text{ Bq g}^{-1} \text{ }^{239/240}\text{Pu}$ and we measured $6.6 \pm 2.0 \text{ Bq g}^{-1} \text{ }^{239/240}\text{Pu}$ (Cadieux et al., 2007). The

246 reagent blank had a trace of $^{239/240}\text{Pu}$ activity, indicating some cross contamination of samples.

247 This slight contamination did not compromise data interpretation.

248

249 **2.3 Numerical Model**

250 A numerical model was used to describe the long term impact that plants may have on Pu
251 concentrations in a lysimeter sediment profile. The model was also used to predict Pu uptake
252 and distribution within the plant (root and shoots). The model included yearly decay of the roots,
253 allowing Pu activity in the root to be transferred back into the sediments at the end of each year.

254 A detailed description of the numerical model is presented in Demirkanli et al. (2007; 2008;
255 2009). We used this existing model for hypothesis testing. Briefly, the fully transient reactive
256 transport modeling of Pu consists of three models, all time-dependent and coupled to each other
257 through various parameters: (1) a variably saturated flow model; (2) a reactive Pu sediment
258 transport model; and (3) a Pu root uptake and xylem transport model. The flow model simulates
259 the time-dependent moisture movement within the sediment core depending on: (1) the daily
260 rainfall data collected during the experiments; (2) root water uptake calculated based on the
261 average monthly temperature; and (3) measured and inferred sediment hydraulic characteristics.

262 The output values of parameters, the velocity and moisture content, for a given time and location
263 within the core are then transferred into the reactive transport model to calculate the Pu
264 movement in the soil core due to reaction, advection, and dispersion. The geochemical processes
265 described by the transport model included two Pu species: a reduced species, Pu(III/IV), and an
266 oxidized species, Pu(V/VI). Kinetic reaction terms were used to describe Pu oxidation and
267 reduction reactions occurring on sediment surfaces. Rate constants for these reactions were used
268 as fitting parameters. Pu(III/IV) and Pu(V/VI) were also assumed to partition to the solid phase

269 using steady-state equilibrium constants. The calculated root water uptake term from the flow
270 model and sediment solution Pu activity concentrations from the reactive transport model were
271 used in the Pu root uptake and transport model to simulate the uptake and Pu transport within the
272 xylem. Pu transport within the xylem occurred by advection and dispersion assuming that the
273 aqueous phase Pu(III/IV) and Pu(V/VI) were transferred into the plant with water uptake. Radial
274 passage between the root-sediment interface and the xylem was assumed to be instantaneous
275 with no sorption to plant material. However, after moving into the xylem, Pu was assumed to
276 sorb onto the xylem wall material of the roots, mainly cellulose, consequently causing
277 retardation. Pu leaving the domain through the top boundary of the root model, i.e., the
278 lysimeter sediment surface, was assumed to be transferred into the above-ground part of the
279 plants (shoots). Yearly senescence of shoots was not included in the initial model.

280

281 **3. Results and discussion**

282

283 **3.1. Plutonium isotopes**

284 Plutonium sediment concentrations and atomic mass fractions of Pu isotopes are presented in
285 Table 1. Not surprisingly, $^{239,240}\text{Pu}$ concentrations were greater than ^{238}Pu . The weapons-grade
286 Pu control sample had about three orders of magnitude greater $^{239,240}\text{Pu}$ concentrations than did
287 the lysimeter surface sediments, except for the surface $\text{Pu}(\text{NO}_3)_4$ sample. The two positive
288 controls for fallout also had low Pu concentrations. ^{239}Pu and ^{240}Pu , the isotopes with the
289 greatest mass fractions, showed less variability between samples than ^{241}Pu and ^{242}Pu (Table 1).
290 Some of the variability of ^{241}Pu may be attributed to its short half life, 14.35 y, relative to the
291 other isotopes: ^{239}Pu ($t_{1/2} = 24,100$ y), ^{240}Pu ($t_{1/2} = 6,560$ y), and ^{242}Pu ($t_{1/2} = 375,000$ y).

292 The atomic mass ratios of $^{242}\text{Pu}/^{239}\text{Pu}$ versus $^{240}\text{Pu}/^{239}\text{Pu}$ are presented in Figure 2. The
293 $^{240}\text{Pu}/^{239}\text{Pu}$ ratio for the weapons-grade Pu control was 0.0634 ± 0.0008 . This value is consistent
294 with Oughton et al. (2000) who reported that weapons-grade Pu generally has a $^{240}\text{Pu}/^{239}\text{Pu}$
295 atomic ratio of <0.07 (2000). $^{240}\text{Pu}/^{239}\text{Pu}$ values for both fallout control samples (0.183 ± 0.002
296 for the Anderson, South Carolina sample and 0.162 ± 0.004 for the Savannah River Site
297 perimeter sample) agreed well with values reported by Kelley et al. (1999) for a soil sample
298 collected in Raleigh, NC; they reported a $^{240}\text{Pu}/^{239}\text{Pu}$ ratio of 0.1811 ± 0.0009 . They also agree
299 with the global fallout average of 0.18 for atmospheric aerosol, soil, and ice core samples (Krey
300 et al., 1976). The large $^{240}\text{Pu}/^{239}\text{Pu}$ difference between the weapons-grade and fallout control
301 samples permits using this atomic ratio to distinguish between these two potential Pu sources.
302 The four lysimeter sediments had very similar $^{240}\text{Pu}/^{239}\text{Pu}$ atomic ratios, ranging from $0.0630 \pm$
303 0.000040 to 0.06354 ± 0.000144 . This range included the weapons-grade Pu control sample
304 (0.06343 ± 0.000823), but not the two fallout control samples. Therefore, this isotopic ratio data
305 indicates that the Pu in the lysimeter surface sediment originated from weapons-grade Pu, the
306 source material used in the lysimeters.

307 $^{242}\text{Pu}/^{239}\text{Pu}$ ratios also provided strong signature differences between the fallout and the
308 weapons-grade Pu used in the lysimeters. $^{242}\text{Pu}/^{239}\text{Pu}$ atomic ratios for the fallout control
309 samples were near identical, about 0.0465, whereas the spike Pu control sample was $0.00051 \pm$
310 $2.5\text{E}-5$, a two order of magnitude difference. Again, this large difference between the two
311 control samples permits using the $^{242}\text{Pu}/^{239}\text{Pu}$ atomic ratios to distinguish between these two
312 potential Pu sources. The $^{242}\text{Pu}/^{239}\text{Pu}$ ratios for the four lysimeter samples ranged between
313 0.000375 to 0.000392 , values strongly indicating the presence of the weapons-grade Pu.

314

315 **3.2. Numerical Modeling**

316 Typical simulations with plant Pu uptake (Simulations 2, 3, and 4) and without plant Pu
317 uptake (Simulation 1) are shown in Figure 3a. Simulations 2, 3, and 4 differ with regards to the
318 partitioning coefficient, K_{d_root} values (Pu concentration ratio of xylem to liquid (sap)), used to
319 calculate Pu retardation in the xylem. As the retardation increases with increasing K_{d_root}
320 partitioning between the xylem solution and xylem material, the amount of Pu retained in the
321 root section increases while the amount being transferred into the shoots/leaves decreases (Figure
322 3b). The model captured the general behavior of the data in the top 20 cm of the lysimeter with
323 the addition of the plant Pu uptake mechanism, except for the scattering which was attributed to
324 the time-dependent and three dimensional growing of the roots by Demirkanli et al. (2009). One
325 of the most important outcomes of these simulations was that the addition of root Pu uptake and
326 xylem transport did not affect the model fit to the below-source portion of the data.

327 As mentioned earlier, Pu leaving from the upper boundary of the root model (top of the
328 lysimeter) was assumed to go into the shoots. As can be seen in Figure 3b, the model predicts
329 that some part of the total activity taken up by the roots is always transferred into the shoots,
330 with the amount being dependent on the retardation in the root xylem. Thus, an accumulation of
331 activity in the surface sediments is expected due to senescence of the Pu containing shoots as
332 seen in the data. Even though the model takes annual decaying of the roots into account and
333 transfers yearly the activity in the roots back into the lysimeter sediment, the activity
334 accumulation in the surface sediment was incorporated into the model only for one simulation,
335 shown in Figure 4, to demonstrate a possible effect of such a mechanism. The simulation in
336 Figure 4 was the same as simulation 3 in Figure 3a with the addition of the transfer of activity in
337 the shoots back into the top sediment yearly, representing the senescence of the leaves. As

338 expected, a mechanism describing leaf senescence may explain the increased concentrations in
339 the lysimeter surface sediment.

340

341 **4. Summary**

342 This study is part of a long term lysimeter program design to provide insight into the fate and
343 transport of Pu in the vadose zone. An unexpected result from this program was that a large
344 proportion of the buried Pu source material had migrated upward. A hypothesis evolved that the
345 surface accumulation of Pu was the result of Pu being taken up by plant roots, translocated to the
346 above-ground portion of the plants, and then deposited as plant detritus on the ground surface
347 (Demirkanli et al., 2009). This hypothesis stemmed from three observations: 1) elevated total Pu
348 concentrations in some surface sediment samples collected at the lysimeter, 2) the intermittent
349 presence of grasses growing on the lysimeters, and 3) modeling results (Demirkanli et al., 2009)
350 suggesting that a substantial amount of Pu could be taken up by lysimeter plants during the 11
351 year experiment.

352 The objective of this study was to determine whether the surface sediment Pu originated from
353 the buried source Pu (weapons-grade Pu) or from atmospheric deposition. This study
354 demonstrated that with out question, the surface Pu had the isotopic signatures of the buried
355 source. This provided additional confirmation that Pu had moved upward. Importantly, this is
356 not direct evidence in support of plant uptake mechanism because that requires plant Pu data for
357 several years. An alternative Pu transport mechanism is that the Pu moved upward as a result of
358 animal activities, such as earth worms or ants. We have chosen to discount this latter mechanism
359 because: 1) the sediment Pu concentration trend data in Figure 1 is too smooth for such
360 bioperturbation transport, 2) the trend lines above the source terms, where animal populations are

361 greatest, are not more perturbed than those below the source terms, and 3) there was not any
362 evidence of animal galleys in the sediment cores. Consequently, in the lack of direct evidence
363 we have collected a preponderance of indirect evidence including computer simulations that have
364 ruled out such factors as evapotranspiration, enhanced Pu oxidation in the vadose zone, enhanced
365 water flow due to hysteresis (Demirkanli et al. 2009); and, new in this manuscript (Figure 3a),
366 we have reasonably simulated the upward sediment Pu concentration experimental data only
367 when we include plant uptake mechanism in our models. Finally, we have also reasonably
368 simulated the accumulation of Pu on surface sediments (Figure 4) by incorporating plant uptake.

369 To our knowledge, this is the first field observation, albeit indirect, of plants facilitating the
370 upward movement of Pu, or any other actinide. In the past, plants were not deemed important
371 transport vectors of actinides because it was repeatedly shown that plants took up very low Pu
372 concentrations with respect to sediment Pu concentrations. Simulations indicate that because
373 plants create a large water flux, small concentrations taken up in the plants over long durations
374 may result in a measurable accumulation of Pu on the ground surface. These results may have
375 implications on the pathway assumed for calculating risk associated with long-term stewardship
376 and monitored natural attenuation management of Pu contaminated subsurface and surface
377 sediments.

378

379 **5. Acknowledgments**

380

381 This project was supported by the following United States Department of Energy programs:
382 Environmental Remediation Science Program (ERSP, within the Office of Science) and South
383 Carolina Universities Research and Education Foundation (SCUREF; "Radiochemistry

384 Education Award Program”). A portion of the work was performed at Clemson University
385 within the Department of Environmental Engineering & Science. Work at the Savannah River
386 National Laboratory (SRNL) was performed under the auspices of the U.S. Department of
387 Energy (DOE) contract DE-AC09-96SR18500.

388

389 **5. References**

390

391 Bais, H.P., Weir, T.L., Perry, L.G., Gilroy, S., Vivanco, J.M., 2006. The Role of root exudates in
392 rhizosphere interactions with plants and other organisms. *Annual Review Plant Biology* 57,
393 233–266.

394 Bar-Ness, E., Hadar, Y., Chen, Y., Shanzer, A., Lobman, J., 1992. Iron uptake by plants from
395 microbial siderophores. *Plant Physiology* 99, 1329–1335.

396 Beasley, R.M., Ball, L.A., Andres, J.E., Halverson, J.E., 1981. Hanford-derived plutonium in
397 Columbia River sediments. *Science* 214, 913–915.

398 Buesseler, K.O., 1997. The isotopic signature of fallout plutonium in the North Pacific. *Journal*
399 *of Environmental Radioactivity* 36, 69–83.

400 Buesseler, K.O., Halverson, J.E., 1987. The mass spectrometric determination of fallout ^{239}Pu
401 and ^{240}Pu in marine samples. *Journal of Environmental Radioactivity* 5, 425–444.

402 Cadieux, J.R., Hall, G, LaMont, S.P., 2007. Detection and measurement of plutonium isotopes in
403 the National Institute of Standards and Technology (NIST)’s Peruvian Soil Standard
404 Reference Material (SRM 4355) by alpha spectrometry and thermal ionization mass

- 405 spectrometry (TIMS). Presented at the 234th National Meeting of the American Chemical
406 Society: Boston, MA Aug., 19th-23rd, 2007.
- 407 Cataldo, D.A., McFadden, K.M., Garland, T.R., Wildung, R.E., 1988. Organic constituents and
408 complexation of nickel(II), iron(III), cadmium(II), and plutonium(IV) in soybean xylem
409 exudates. *Plant Physiology* 86, 734–739.
- 410 Demirkanli, D.I., Molz, F. J., Kaplan, D.I., Fjeld, R. A., Serkiz, S.M., 2007. Long-term vadose
411 zone plutonium transport at the Savannah River National Laboratory. *Vadose Zone Journal* 6,
412 344–352.
- 413 Demirkanli, D.I., Molz, F. J., Kaplan, D.I., Fjeld, R.A., Serkiz, S.M., 2008. A fully transient
414 model for long-term plutonium transport in the Savannah River Site vadose zone: plant water
415 uptake. *Vadose Zone Journal* 7, 1099–1109.
- 416 Demirkanli, D.I., Molz, F.J., Kaplan, D.I., Fjeld, R.A., 2009. Soil-root interactions controlling
417 upward plutonium transport in variably saturated soils. *Vadose Zone Journal* 9, 574–585.
- 418 Halverson, J.E., 1981. A Three-State Mass Spectrometer for Isotope Analysis of Radionuclides
419 in Environmental Samples. DP-1611. E. I. du Pont de Nemours and Co., Aiken, SC.
- 420 Harley, J. H., 1980. Plutonium in the environment – A review. *Journal of Radiation Research* 21,
421 83–104.
- 422 Kaplan, D.I., Demirkanli, D.I., Gumapas, L., Powell, B.A., Fjeld, R.A., Molz, F.J., Serkiz, S.M.,
423 2006. 11-year field study of Pu migration from Pu III, IV, and VI sources. *Environmental*
424 *Science and Technology* 40, 443–448.

- 425 Kaplan, D.I., Powell, B.A., Demirkanli, D.I., Fjeld, R.A., Molz, F.J., Serkiz, S.M., Coates, J.T.,
426 2004. Enhanced plutonium mobility during long-term transport through an unsaturated
427 subsurface environment. *Environmental Science and Technology* 38, 5053–5058.
- 428 Kaplan, D.I., Powell, B.A., Duff, M.C., Demirkanli, D.I., Denham, M., Fjeld, R.A., Molz, F. J.,
429 2007. Plutonium source solubilities and oxidation state transformations in vadose zone
430 sediments. *Environmental Science and Technology* 41(21), 7417–7423.
- 431 Kelley, J.M., Bond, L.A., Beasley, T.M., 1999. Global distribution of Pu isotopes and ^{237}Np .
432 *Science of the Total Environment* 237/238, 483–500.
- 433 Koide, M., Bertine, K.K., Chow, T.J., Goldberg, E.D., 1983. The $^{240}\text{Pu}/^{239}\text{Pu}$ ratio, a potential
434 geochronometer. *Earth Planet Science Letters* 72, 1–8.
- 435 Krey, P.W., Hardy, E.P., Pachucki, C., Rourke, F., Coluzza, J., Benson, W. K., 1976. Mass
436 Isotopic Composition of Global Fall-Out Plutonium in Soil. In: *Transuranium Nuclides in the*
437 *Environment*. IAEA-SM-199/39, 671–678. IAEA, Vienna.
- 438 Landa, E.R., Reimnitz, E., Beals, D.M., Pochkowski, J.M., Winn, W.G., Rigor, I., 1998.
439 Transport of ^{137}Cs and $^{239,240}\text{Pu}$ with ice-rafted debris in the Arctic Ocean. *Arctic*. 51, 27–39.
- 440 Oughton, D.H., Fifield, L.D., Day, J.P., Skipperud, L., Di Tada, M.L., Salbu, B., Strand, P.,
441 Drozcho, E., Mokrov, Y., 2000. Plutonium from Mayak: measurement of isotope ratios and
442 activities using accelerator mass spectrometry. *Environmental Science and Technology* 34,
443 1938–1945.
- 444 Perkins, R.W., Thomas, C.W., 1980. Worldwide fallout. In *Transuranic Element in the*
445 *Environment*, Hanson, W.D. (Ed.), Technology Information Center U.S. Department of
446 Energy: Washington, DC, pp. 53–82.

- 447 Powell, B.A., Fjeld, R.A., Kaplan, D.I., Coates, J.T., Serkiz, S.M., 2005. Pu(V)O₂⁺ absorption
448 and reduction by synthetic hematite and goethite. *Environmental Science and Technology* 39,
449 2107–2114.
- 450 Rengel, Z., Romheld, V., 2000. Root exudation and Fe uptake and transport in wheat genotypes
451 differing in tolerance to Zn deficiency. *Plant and Soil* 222, 25–34.
- 452 Riley, R.G., Zachara, J.M., 1992. Chemical Contaminants on DOE Lands and Selection of
453 Contaminant Mixtures for Subsurface Science Research. DOE/ER-0547T. U.S. Department of
454 Energy, Washington, DC.
- 455 Romney, E.M., Mork, H.M., Larson, K.H., 1970. Persistence of plutonium in soil, plants, and
456 small mammals. *Health Physics* 19, 487–491.
- 457 Sanford, W.E., Larsen, I.L., McConnell, J.W., Rogers, R.D., 1998. Upward migration of radio-
458 cesium and strontium in a sand-filled lysimeter. *Journal of Environmental Radioactivity* 41,
459 147–162.
- 460 Silva, R.J., Nitsche, H., 1995. Actinide environmental chemistry. *Radiochimica Acta* 70/71,
461 377–396.
- 462 Wang, Y.Y., Biber, B.M., Yu, C., 1993. A Compilation of Radionuclide Transfer Factors for the
463 Plant, Meat, Milk and Aquatic Food Pathways and the Suggested Default Values for the
464 RESRAD code. ANL/EAIS/TM-103, Argonne National Laboratory, Argonne, IL.
- 465 Wildung, R.E., Garland, T.R., 1974. Influence of soil plutonium concentration on plutonium
466 uptake and distribution in shoots and roots of barley. *Journal of Agricultural Food Chemistry*
467 22(5), 836–838.

468 **List of Figures**

469 Fig. 1. Total Pu sediment concentrations in three lysimeters left exposed to natural weather
470 conditions for 11 years.

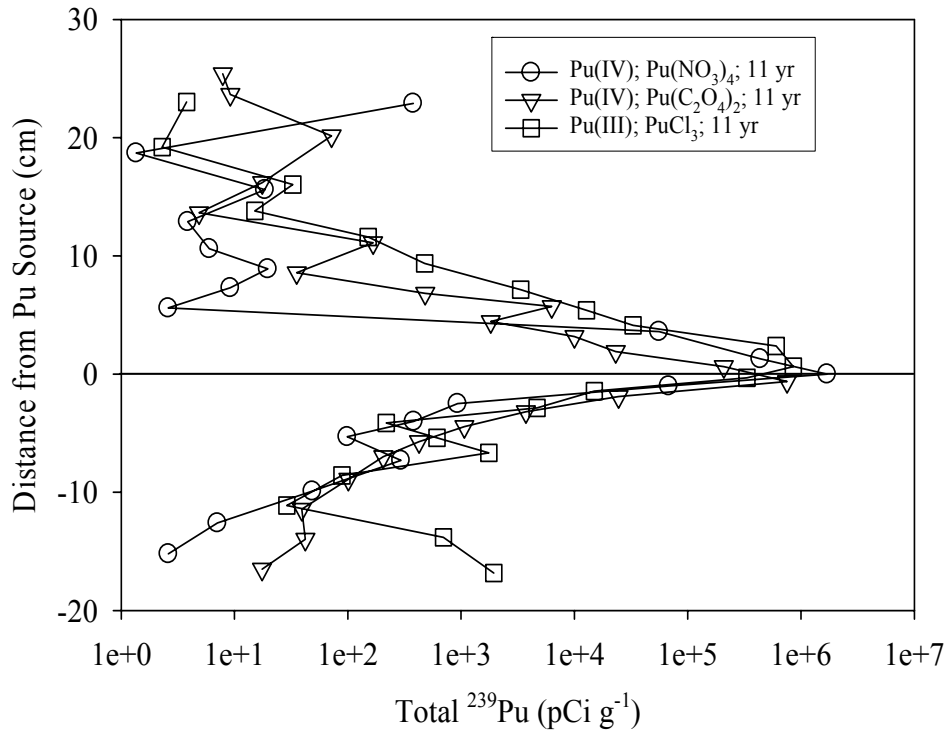
471
472 Fig. 2. Atomic ratios of $^{242}\text{Pu}/^{239}\text{Pu}$ versus $^{240}\text{Pu}/^{239}\text{Pu}$ for the four lysimeter surface sediment
473 samples, two fallout control samples collected 16 and 190 km from the study site, and a positive
474 control for the weapons-grade Pu used as spike material in the lysimeters. The larger graph
475 demonstrates that the Pu isotopic ratios of the surface lysimeter sediments differ greatly from
476 fallout control samples. Inserted graph demonstrates that the lysimeter surface sediments had
477 similar isotopic ratios as a weapons-grade Pu control sediment.

478
479 Fig. 3. (a) Simulations with and without Pu root uptake and xylem transport and varying Pu-root
480 distribution coefficient values (K_{d_root}). (b) Activity distribution within different parts of the plant
481 compared to the amount taken up into the plant and returned into the lysimeter sediment due to
482 the yearly root decay. S/S_o is the activity concentration (S) in the sediment/root system divided
483 by the activity concentration at the source location (S_o). K_{d_root} is the partitioning coefficient in
484 the xylem between the xylem solution and xylem wall material.

485
486 Fig. 4. This is the same simulation as Simulation 3 in Figure 3a with the addition of the transfer
487 of activity in the shoots back into the top sediment yearly. S/S_o is the Pu concentration (S) in the
488 sediment/root system divided by the Pu concentration at the source location (S_o). K_{d_root} is the
489 partitioning coefficient in the xylem between the xylem solution and xylem wall material.

490 Symbols represented measured values.

491

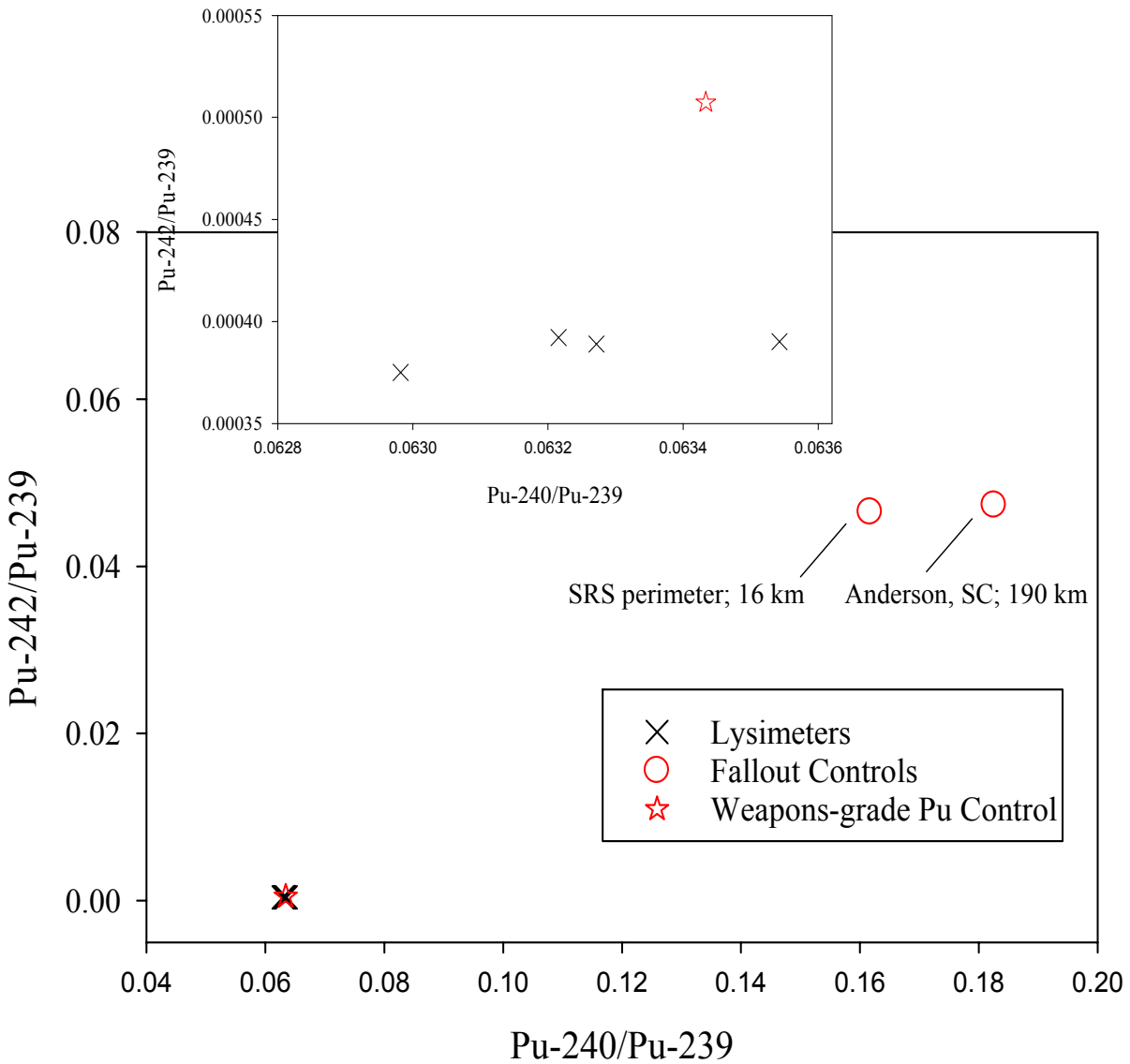


492

493

494 **Fig. 1. Total Pu sediment concentrations in three lysimeters left exposed to natural**
495 **weather conditions for 11 years.**

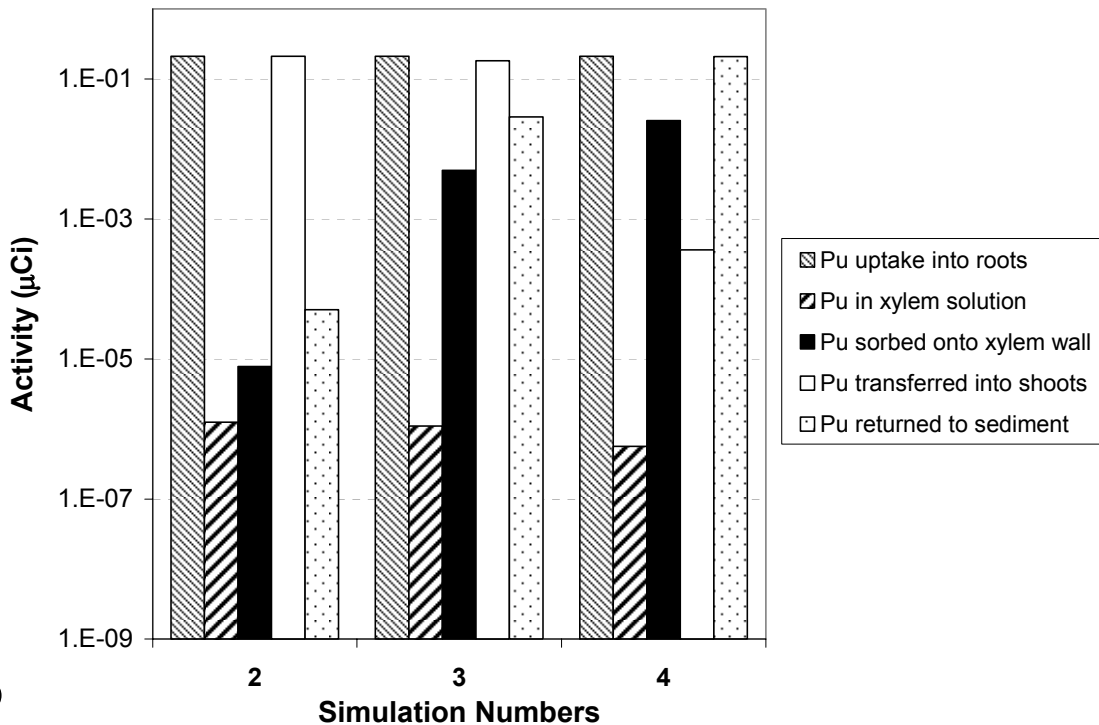
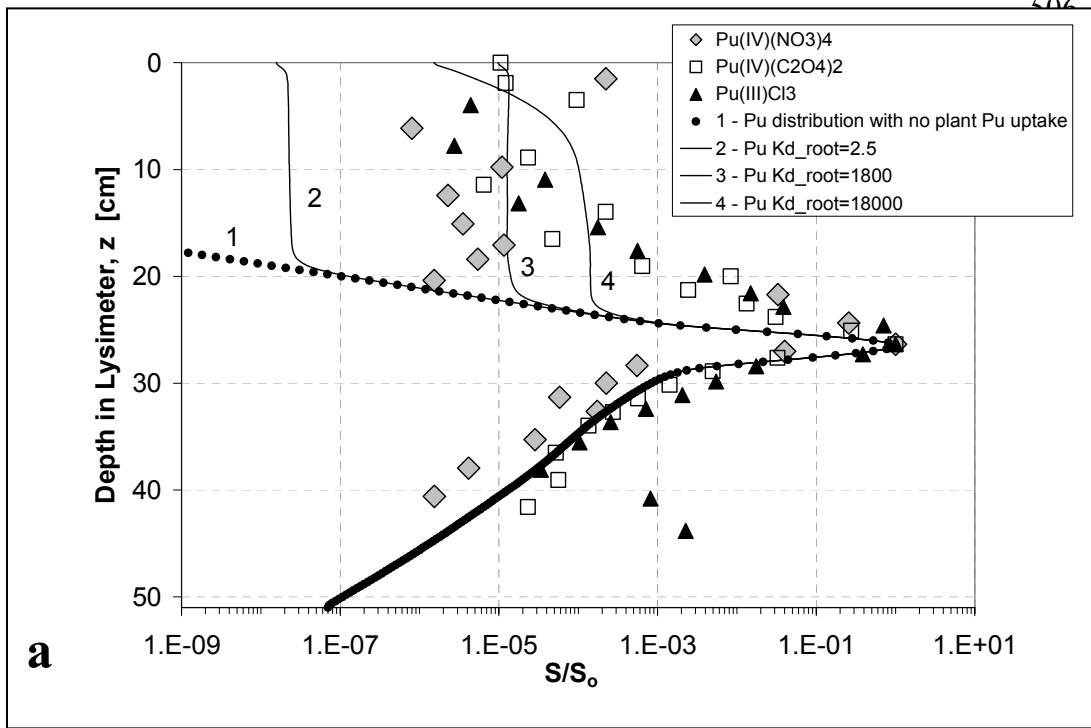
496



497

498

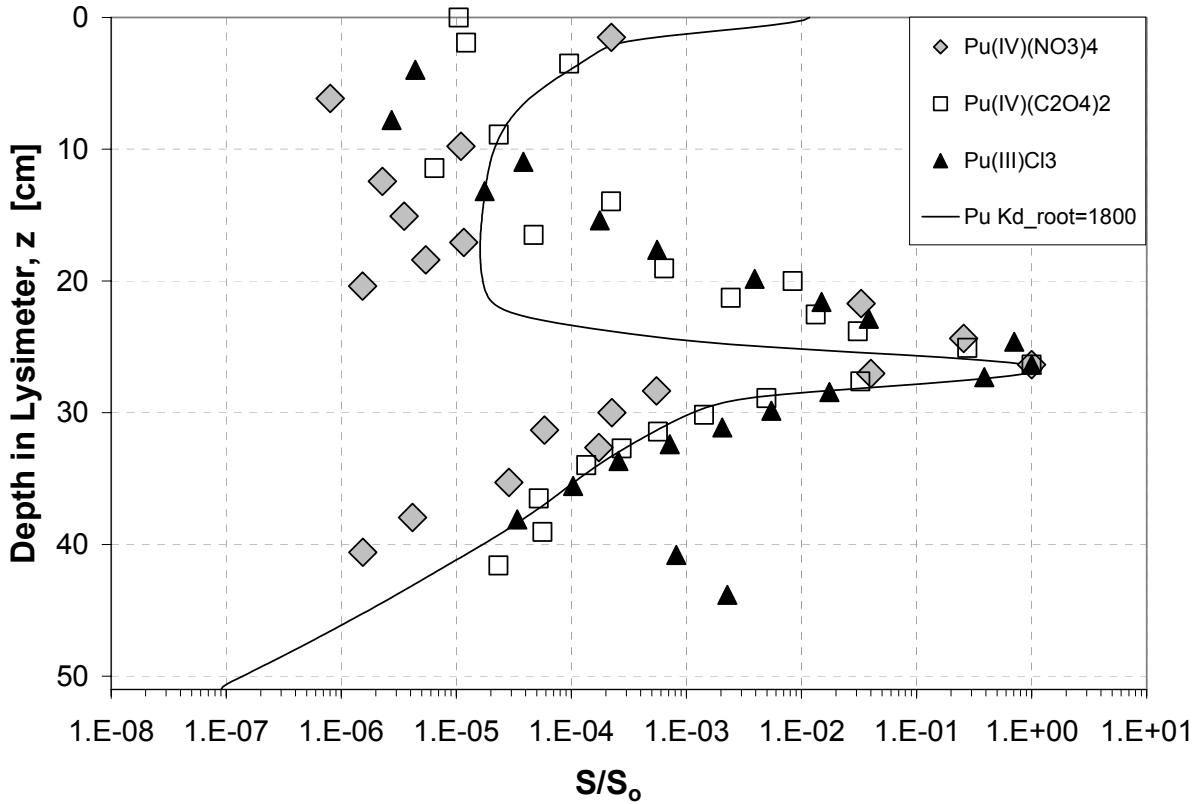
499 **Fig. 2. Atomic ratios of $^{242}\text{Pu}/^{239}\text{Pu}$ versus $^{240}\text{Pu}/^{239}\text{Pu}$ for the four lysimeter surface**
500 **sediment samples, two fallout control samples collected 16 and 190 km from the study site,**
501 **and a positive control for the weapons-grade Pu used as spike material in the lysimeters.**
502 **The larger graph demonstrates that the Pu isotopic ratios of the surface lysimeter**
503 **sediments differ greatly from fallout control samples. Inserted graph demonstrates that**
504 **the lysimeter surface sediments had similar isotopic ratios as a weapons-grade Pu control**
505 **sediment.**



526
 527
 528
 529
 530
 531
 532

FIG. 3. (a) Simulations with and without Pu root uptake and xylem transport and varying Pu-root distribution coefficient values (K_{d_root}). **(b)** Activity distribution within different parts of the plant compared to the amount taken up into the plant and returned into the lysimeter sediment due to the yearly root decay. S/S_0 is the activity concentration (S) in the sediment/root system divided by the activity concentration at the source location (S_0). K_{d_root} is the partitioning coefficient in the xylem between the xylem solution and xylem wall material.

533



534

535 **Fig. 4.** This is the same simulation as Simulation 3 in Figure 3a with the addition of the
536 transfer of activity in the shoots back into the top sediment yearly. S/S₀ is the Pu
537 concentration (S) in the sediment/root system divided by the Pu concentration at the
538 source location (S₀). K_d_root is the partitioning coefficient in the xylem between the xylem
539 solution and xylem wall material. Symbols represented measured values.

540

541

Table 1. Pu isotope activity and atomic mass fractions in samples and controls.

Sample	²³⁸ Pu	^{239,240} Pu	²³⁹ Pu		²⁴⁰ Pu		²⁴¹ Pu	
	conc. (Bq g ⁻¹)	conc. (Bq g ⁻¹)	fraction	2 sigma	fraction	2 sigma	fraction	2 sigma
Pu(C ₂ O ₄) ₂ Lysimeter	<0.10	0.30	0.9386	0.0006	0.059331	6.2488E-05	0.001763	5.99E-05
Pu(NO ₃) ₄ Lysimeter	0.25	13.98	0.9388	0.0003	0.059125	3.2043E-05	0.001762	3.08E-05
PuCl ₃ Lysimeter	0.08	0.13	0.9385	0.0007	0.059379	7.1694E-05	0.001779	6.90E-05
Pu(OH) ₄ Lysimeter	<0.10	0.15	0.9382	0.0011	0.059617	1.1617E-04	0.001794	1.12E-04
WG-Pu Source Control ^(a)	0.25	14.15	0.9382	0.0006	0.059658	6.5478E-05	0.001791	6.30E-05
Fallout Control-16 km ^(b)	2.59E-5	3.737E-4	0.8596	0.0112	0.1390	2.6E-3	0.0015	0.0001
Fallout Control-180 km ^(b)	<1.11e-5	4.551E-4	0.8446	0.0041	0.1542	1.1E-3	0.0012	0.0001

^(a) WG-Pu Source Control = Weapons-grade Pu source material

^(b) Fallout Controls were collected from the perimeter of the SRS, Aiken, SC USA located 16 km from the lysimeter site and from Andromeda, SC USA located 180 km from the lysimeter site, respectively.

^(c) ²⁴²Pu concentrations are not available for these samples because this isotope was added to provide percent Pu recovery data. This yield was determined using a mass spectrometer to provide Pu concentration data. The "0.04 value" was taken from Kelley et al. (1999), for a sample collected in R. 1999.

542

543

544